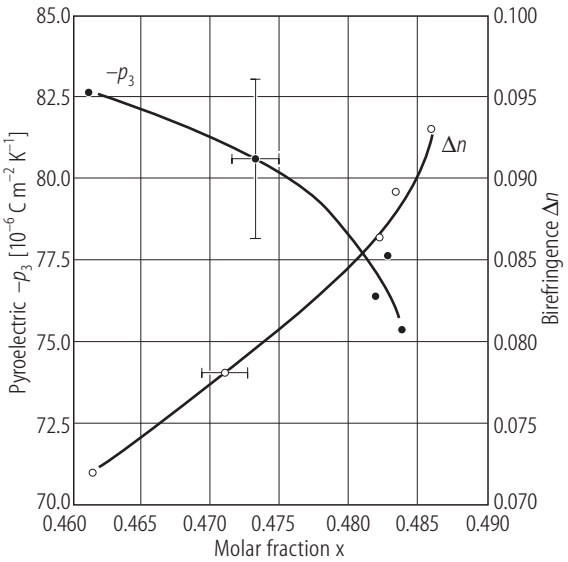

Fig. 2A-1-070. $LiNbO_3$. $-p_3$, Δn vs. x [91Gra]. x: Li_2O content.

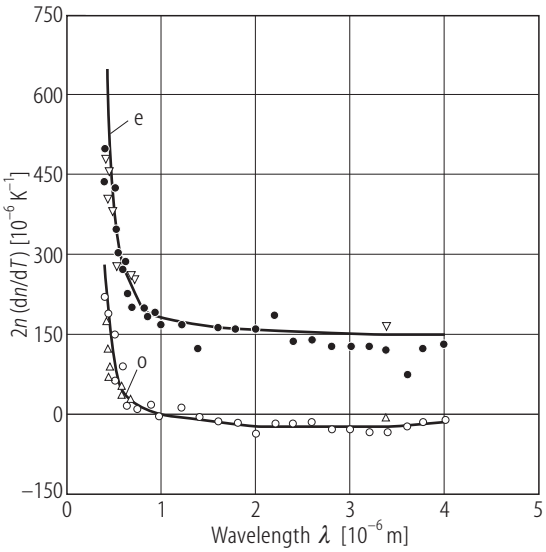

Fig. 2A-1-071. $LiNbO_3$. $2n(dn/dT)$ vs. λ [94Gho]. o: ordinary; e: extraordinary.

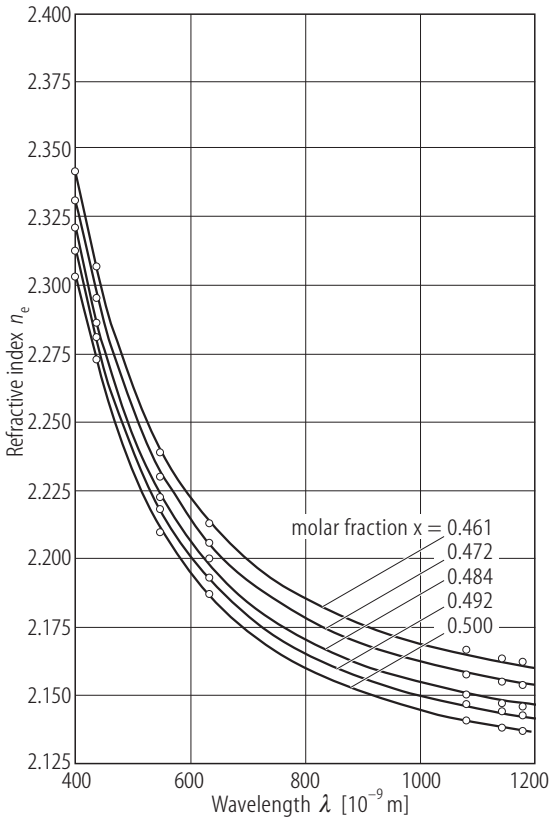

Fig. 2A-1-072. $LiNbO_3$. n_e vs. λ [93Sch1]. Parameter x: Li content.

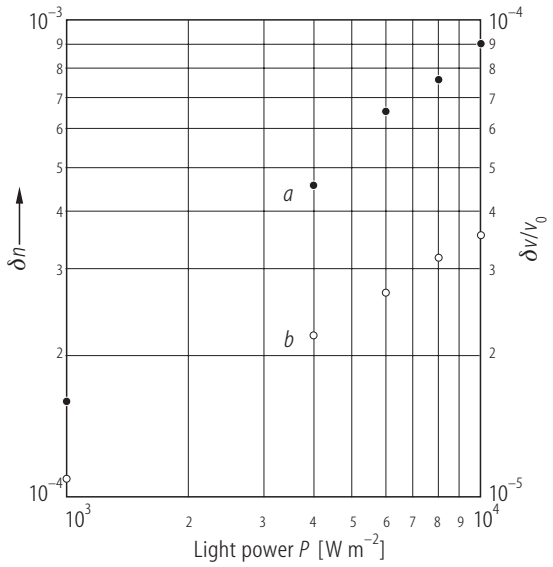

Fig. 2A-1-073. $LiNbO_3$. δn, $\delta v/v_0$ vs. P [92Vla]. δn: change in refractive index; $\delta v/v_0$: fractional change in ultrasound velocity; P: light power for sample illumination.

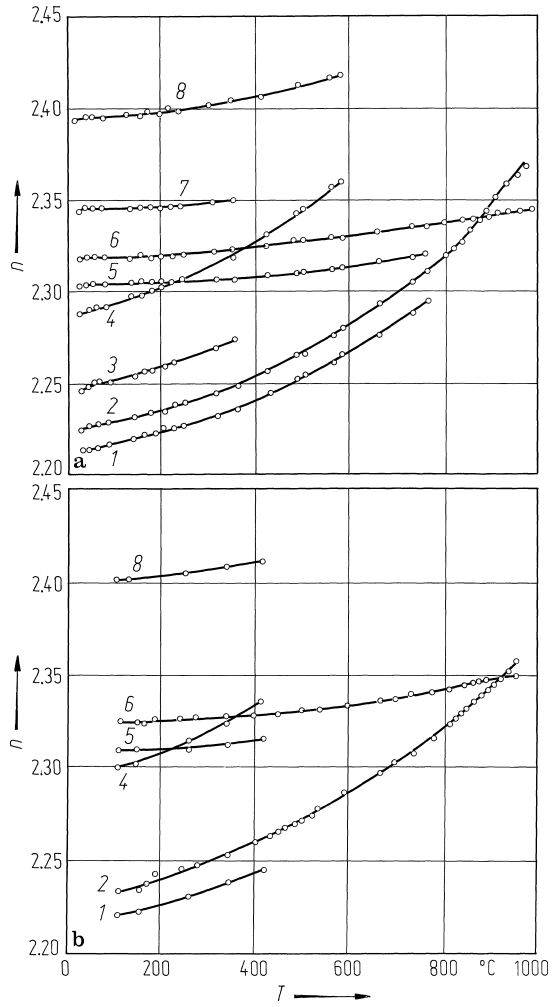

Fig. 2A-1-074. $LiNbO_3$. *n* vs. *T* [79Sir]. (**a**) pure $LiNbO_3$, (**b**) $LiNbO_3$ with the addition of 0.1 mol % Ti. Curves *1...4*: n_e , *5...8*: n_o. *1*, *5*: λ = 585 nm; *2*, *6*: λ = 546 nm; *3*, *7*: λ =480 nm; *4*, *8*: λ = 405 nm.

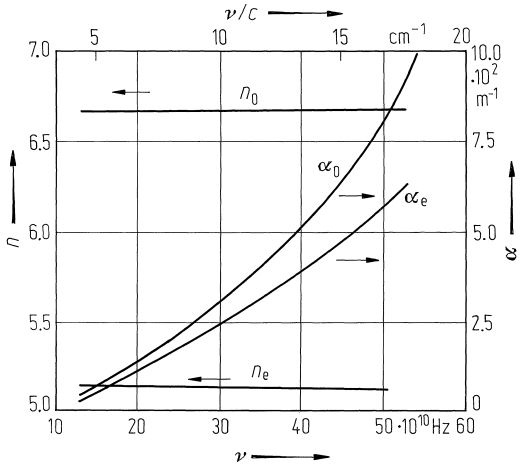

Fig. 2A-1-075. $LiNbO_3$. n, α vs. ν in the near millimeter wave region [83Bro]. α: power absorption coefficient.

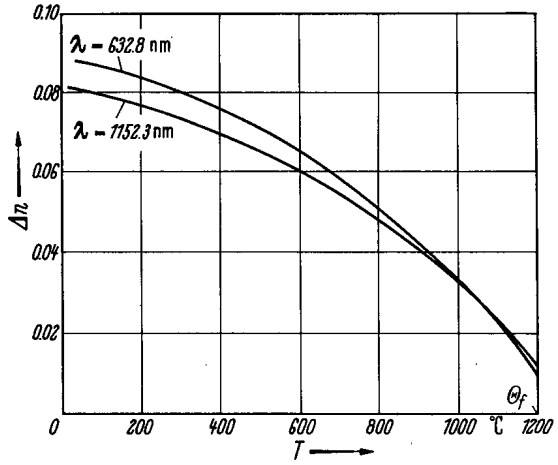

Fig. 2A-1-076. $LiNbO_3$. Δn vs. T [66War]. $\Delta n = n_o - n_e$. Parameter: λ.

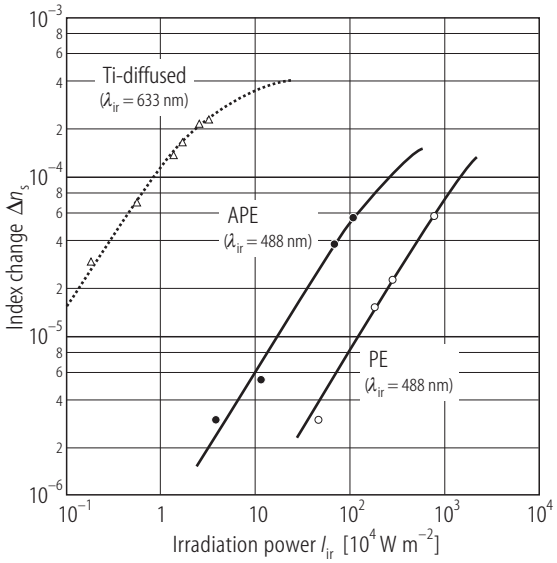

Fig. 2A-1-077. $LiNbO_3$. Δn_s vs. I_{ir} [93Fuj]. Δn_s: saturated refractive index change; I_{ir}: irradiation laser power. Ti-diffused: Ti-diffused sample; PE: proton-exchanged sample; APE: annealed proton-exchanged sample.

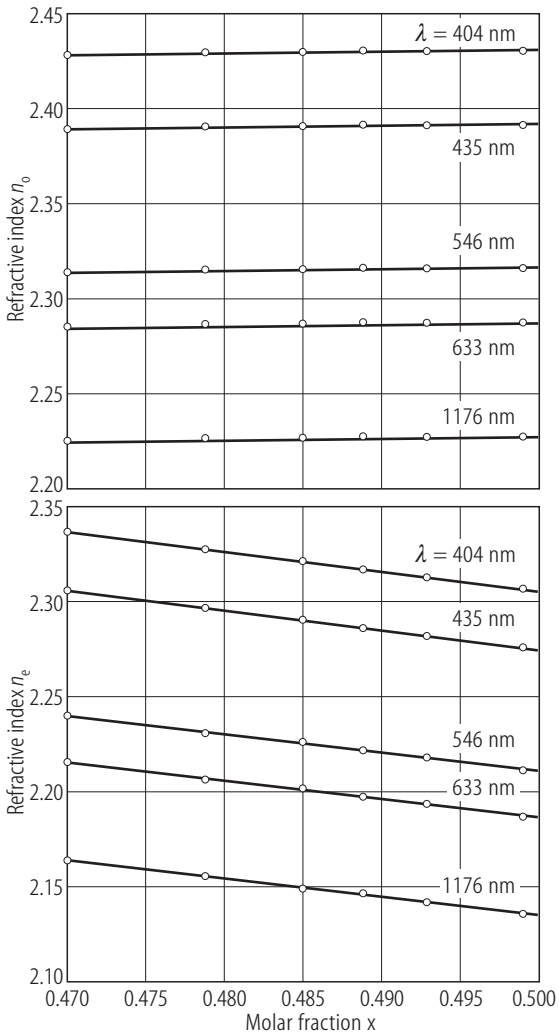

Fig. 2A-1-078. $LiNbO_3$. n_o, n_e vs. x [94Sch]. x: Li_2O content. Parameter: λ.

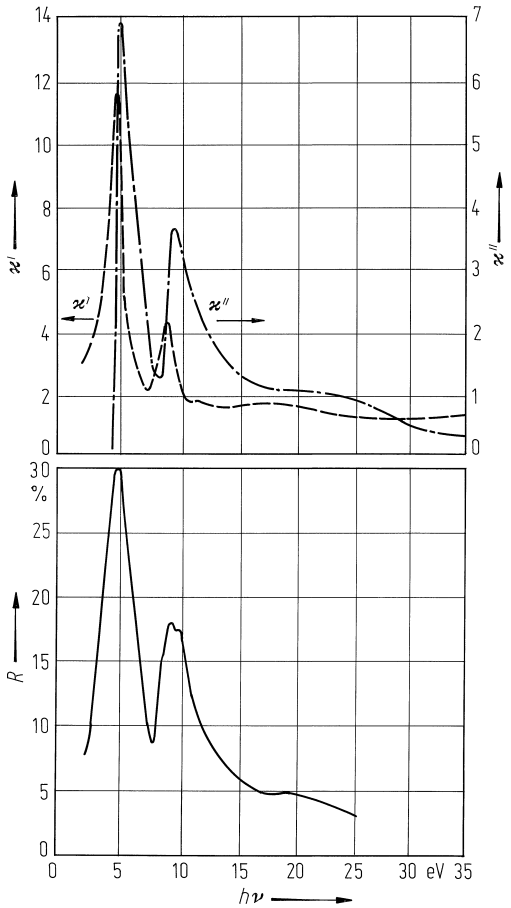

Fig. 2A-1-079. $LiNbO_3$. R, κ', κ'' vs. $h\nu$ at 300 K [83Mam]. $h\nu$: photon energy. R: reflectivity.

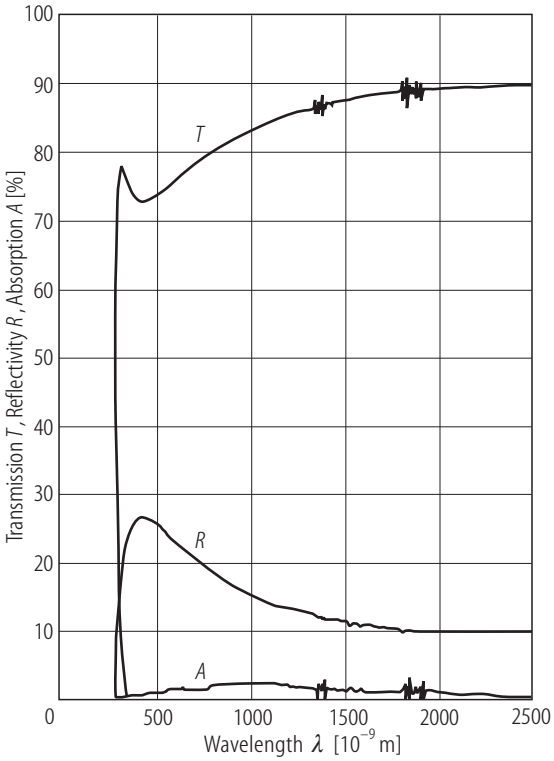

Fig. 2A-1-080. $LiNbO_3$ (thin film). *T*, *R*, *A* vs. λ [92Ben]. Sample: thin film prepared by RF sputtering. *T*, *R*, *A*: transmission, reflectivity and absorption of the light. d = 85 nm.

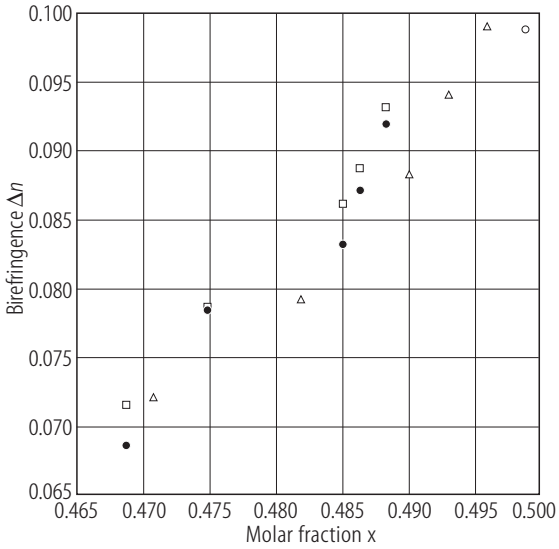

Fig. 2A-1-081. $LiNbO_3$. Δn vs. x [92Sch]. Δn: $n_o - n_e$; x: Li_2O content. Open circles, squares, triangles, full circles: samples of different origins.

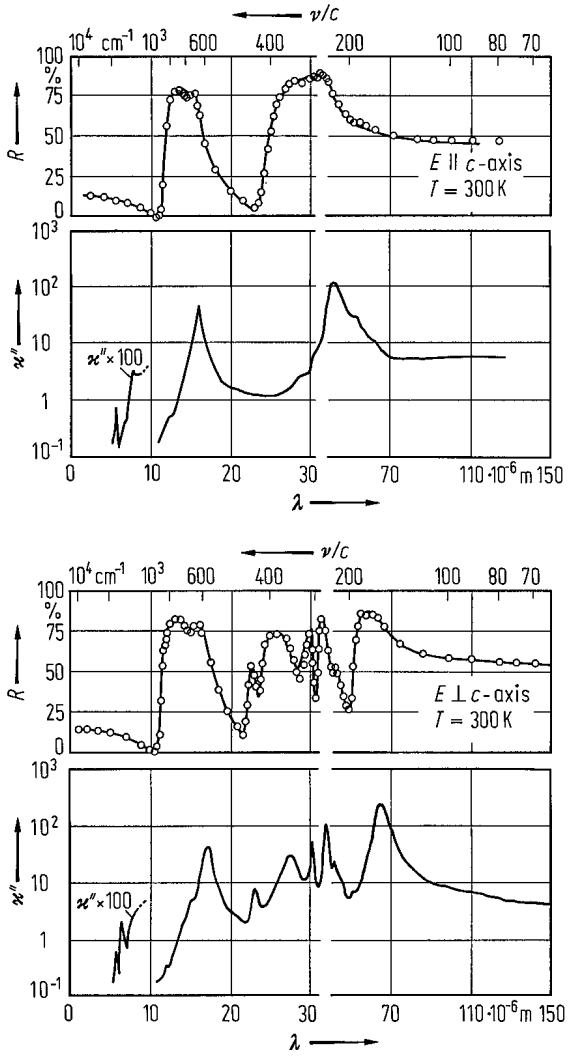

Fig. 2A-1-082. $LiNbO_3$. R, κ'' vs. λ [67Bar]. R: reflectivity. κ'' for $\lambda > 10 \cdot 10^{-6}$ m results from Kramers-Kronig relations; for $10 \cdot 10^{-6}\text{m} > \lambda > 5 \cdot 10^{-6}\text{m}$, κ'' is deduced from transmission measurement.

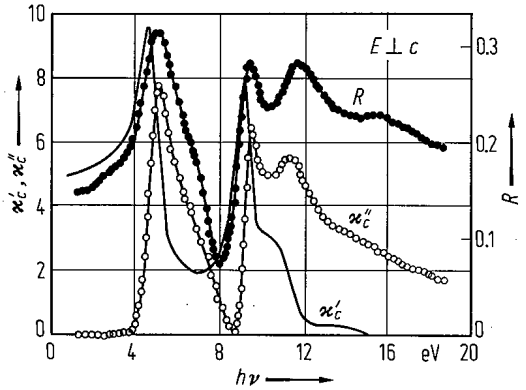

Fig. 2A-1-083. $LiNbO_3$. R, κ_c', κ_c'' vs. $h\nu$ [75Vis]. R: reflectivity.

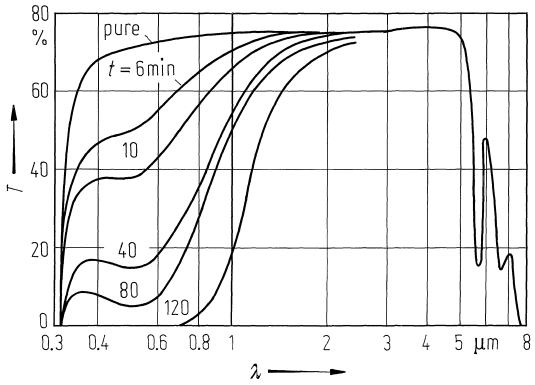

Fig. 2A-1-084. $LiNbO_3$ (pure and reduced). T vs. λ [86Jha]. T: transmission. Parameter: heat treatment time in H_2 at 830 K. Sample thickness is 50 µm.

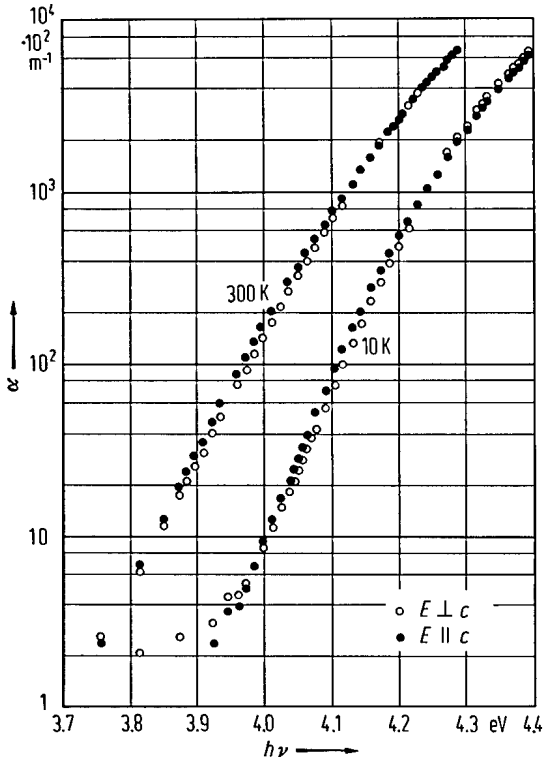

Fig. 2A-1-085. $LiNbO_3$. α vs. $h\nu$ [75Wea]. α: optical absorption coefficient. The crystal was grown from a congruent melt. See also [74Red].

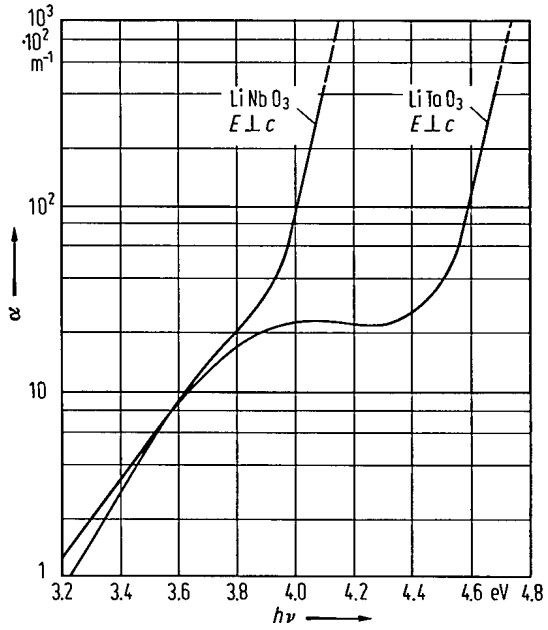

Fig. 2A-1-086. $LiNbO_3$, $LiTaO_3$. α vs. $h\nu$ [74Kas]. α: optical absorption coefficient.

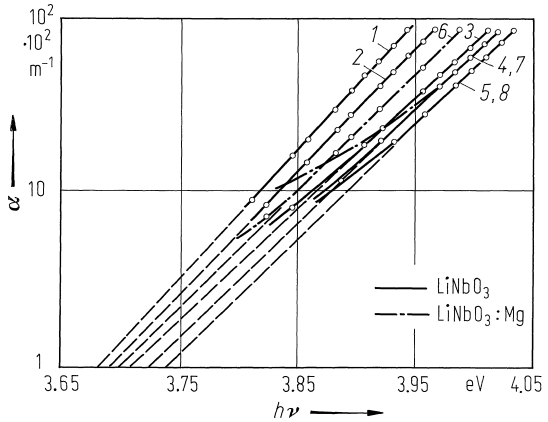

Fig. 2A-1-087. $LiNbO_3$ (undoped and MgO-doped). α vs. $h\nu$ [86Fen]. α: optical absorption coefficient. $h\nu$: photon energy. Parameter: composition. Curve *1*: [Li] / [Nb] = 0.90. *2*: 0.945. *3*: 1.00. *4*: 1.04. *5*: 1.083. *6*: 0.945. *7*: 1.00. *8*: 1.04. Curves *6*, *7* and *8*: additionally 1.0 mol % MgO.

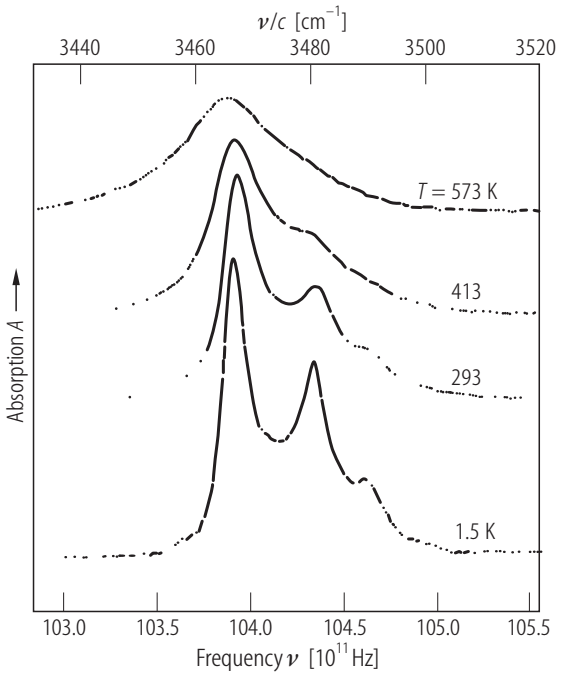

Fig. 2A-1-088. $LiNbO_3$. *A* vs. ν [91Kov]. *A*: absorption. OH absorption bands. Parameter: *T*.

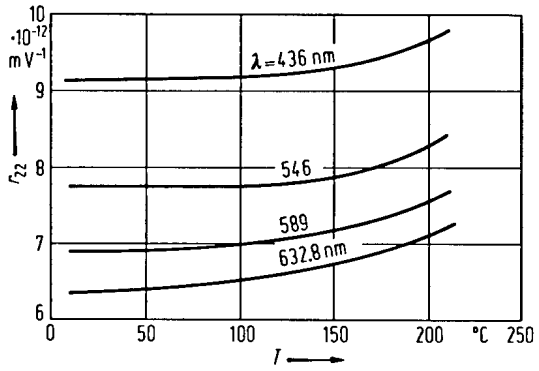

Fig. 2A-1-089. $LiNbO_3$. r_{22} vs. T [68Iwa]. Parameter: λ.

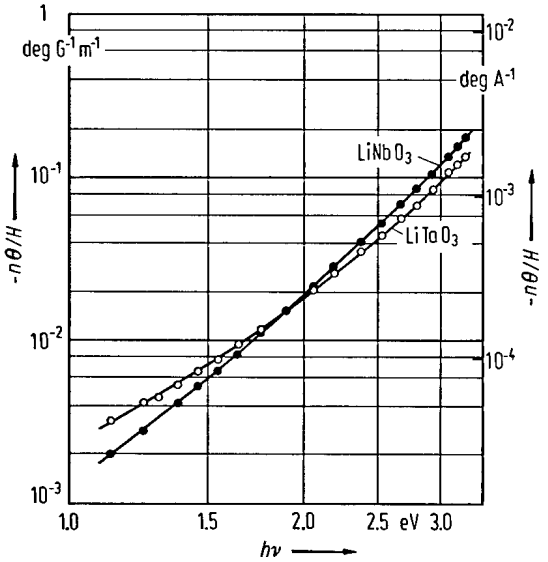

Fig. 2A-1-090. $LiNbO_3$, $LiTaO_3$. $-n\theta/H$ vs. $h\nu$ [74Kas]. n: refractive index, θ: Faraday rotation per unit length, H: magnetic field strength.

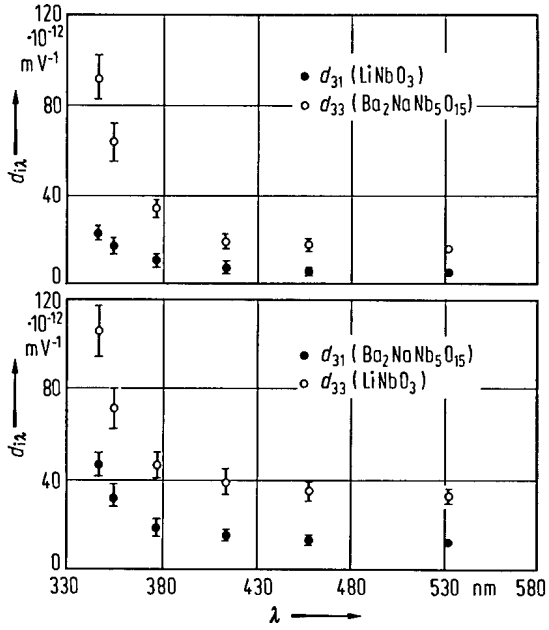

Fig. 2A-1-091. $LiNbO_3$, $Ba_2NaNb_5O_{15}$. $d_{i\lambda}$ vs. λ [76Dor].
$d_{i\lambda}$: nonlinear optical susceptibility.

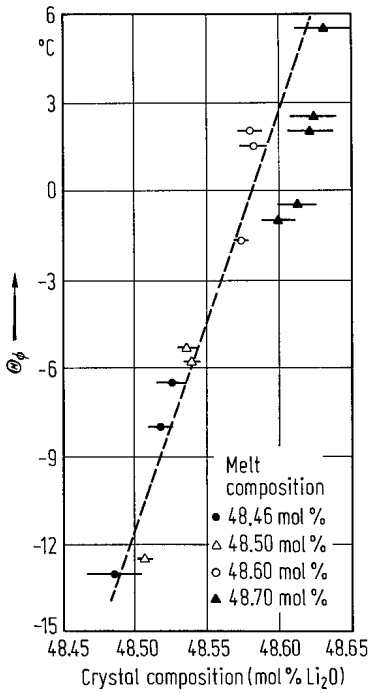

Fig. 2A-1-092. $LiNbO_3$. Θ_ϕ vs. crystal composition [74Cho]. Θ_ϕ: phase matching temperature in optical second harmonic generation.

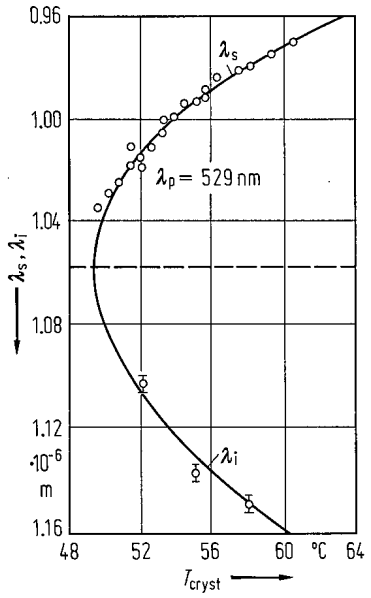

Fig. 2A-1-093. $LiNbO_3$. λ_s, λ_i vs. T_{cryst} [65Gio]. λ_s, λ_i: wavelengths of signal and idler light in parametric oscillation. T_{cryst}: phase matching crystal temperature, λ_p: wavelength of pump light obtained as the second harmonic of a Nd-doped $CaWO_4$ laser.

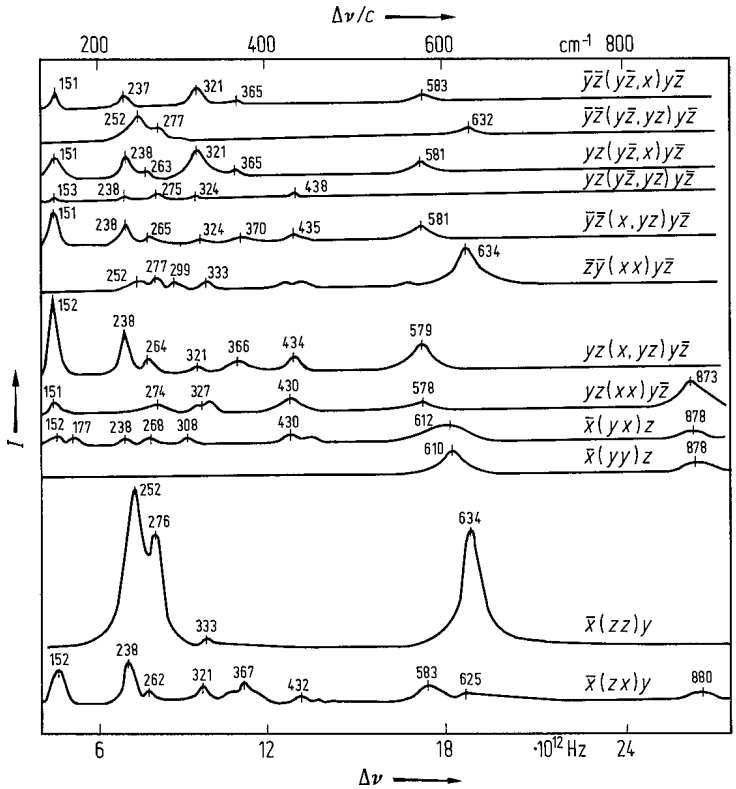

Fig. 2A-1-094. $LiNbO_3$. I vs. $\Delta\nu$ at RT [67Bar]. I: Raman scattering intensity, $\Delta\nu$: frequency shift. The numbers in the figure indicate the peak frequencies in the units of cm^{-1}. See also [66Sch].

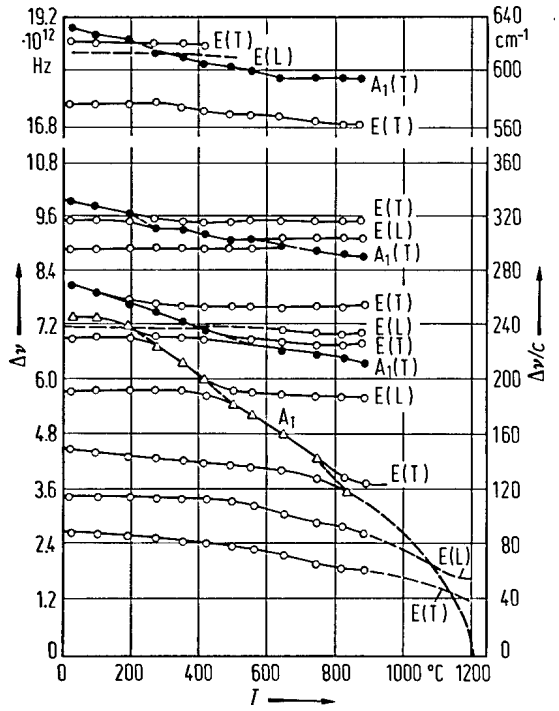

Fig. 2A-1-095. $LiNbO_3$. $\Delta\nu$ vs. T [68Joh]. $\Delta\nu$: Raman frequency shift. Triangles indicate the soft-mode peak. Broken lines are mere extrapolation of the data. For the assignment of the modes, see Table 2A-1-023.

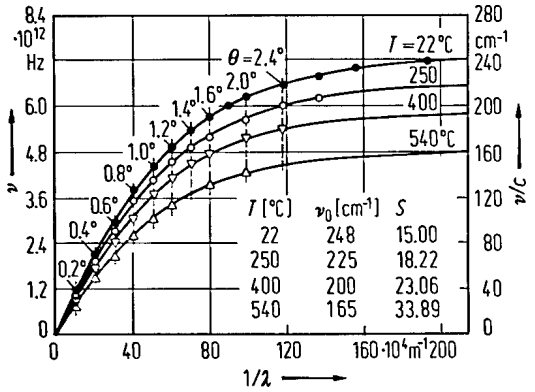

Fig. 2A-1-096. $LiNbO_3$. ν vs. $1/\lambda$ [72Rok]. ν: frequency of polariton associated with the 248 cm^{-1} soft mode, $1/\lambda$: wave number of polariton. θ: scattering angle. The mode frequency ν_0 and the mode strength S are also indicated in the figure.

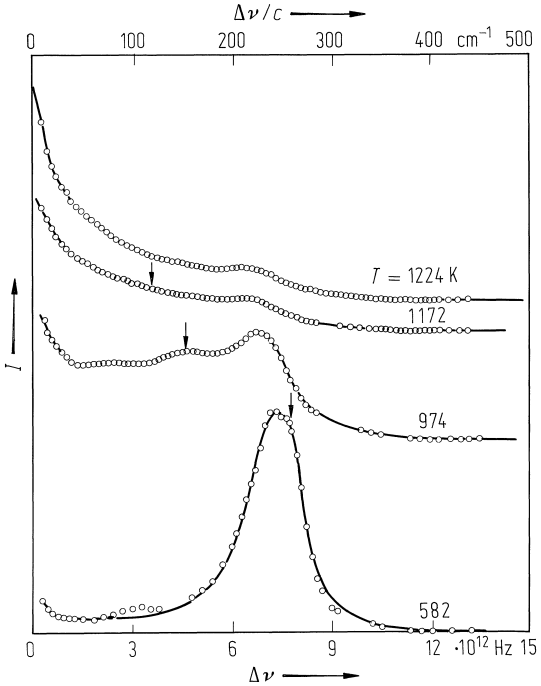

Fig. 2A-1-097. $LiNbO_3$. I vs. $\Delta\nu$ [85Oka]. I: Raman scattering intensity for cc polarizability, $\Delta\nu$: Raman scattering frequency shift. Parameter: T. Arrow on each trace marks the position of soft mode frequency.

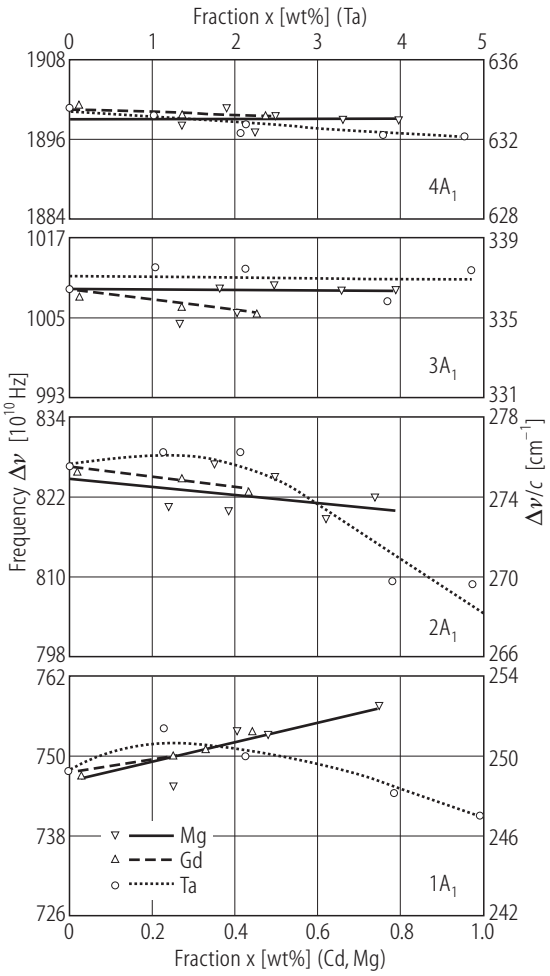

Fig. 2A-1-098. $LiNbO_3$ (Mg, Gd, Ta-doped). $\Delta\nu$ vs. x [94Sid]. $\Delta\nu$: Raman shift. x: wt% concentration.

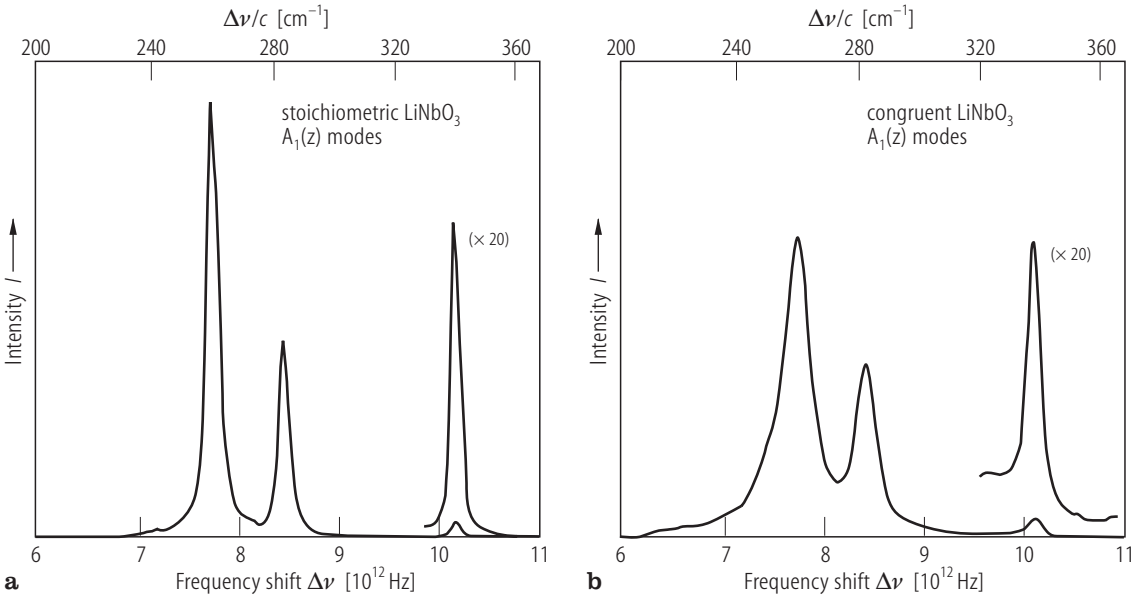

Fig. 2A-1-099. $LiNbO_3$. Raman spectra of $A_1(z)$ modes [94Koj]. (**a**): stoichiometric; (**b**): congruent crystal. T = 95 K.

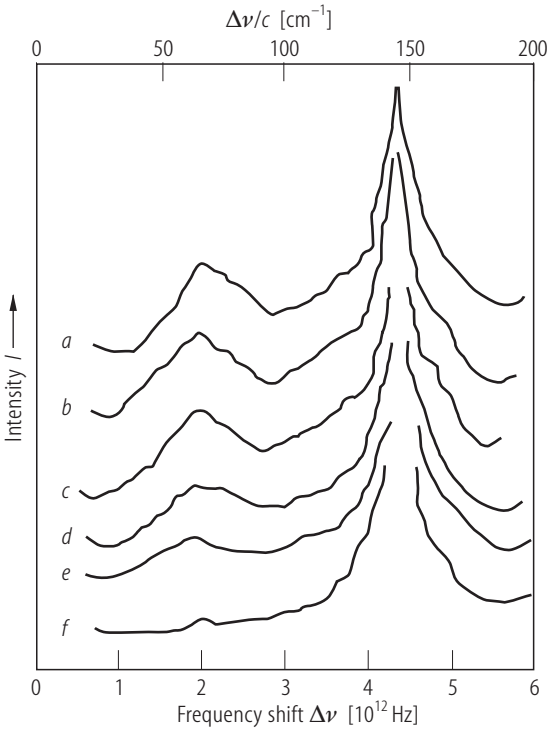

Fig. 2A-1-100. $LiNbO_3$. Raman spectra from a proton-exchanged waveguide [92Sav]. Curve *a*: after the proton-exchange, *b*, *c*, *d*, *e*: after consecutive polishings of very thin layers from the surface, *f*: bulk spectrum.

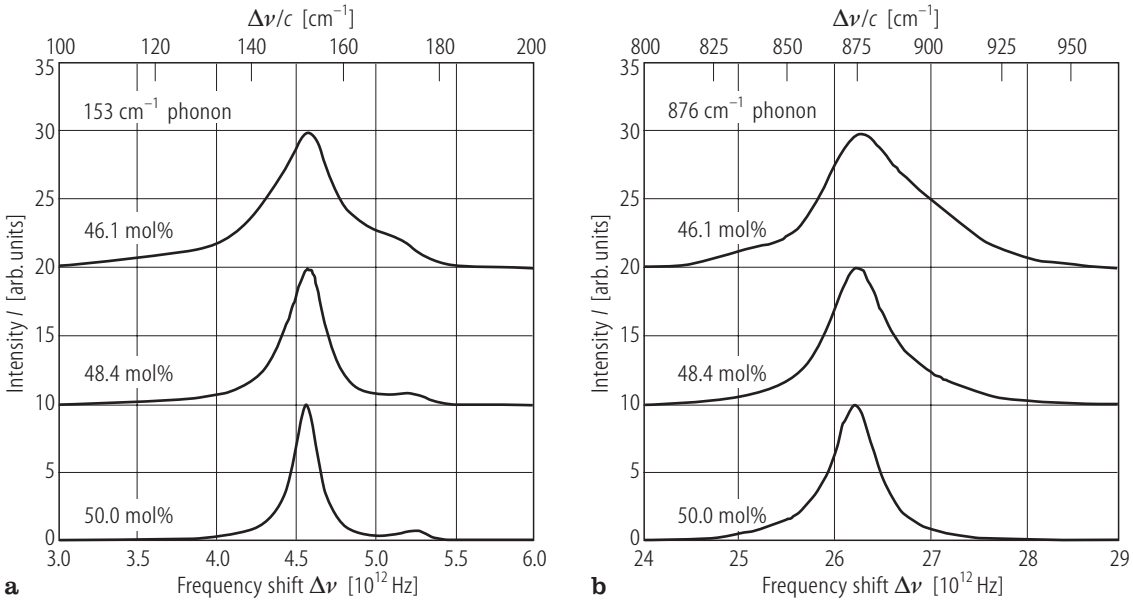

Fig. 2A-1-101. $LiNbO_3$. I vs. $\Delta\nu$ [93Sch2]. I: Raman intensity. $\Delta\nu$: frequency shift. Parameter: Li content [mol%].

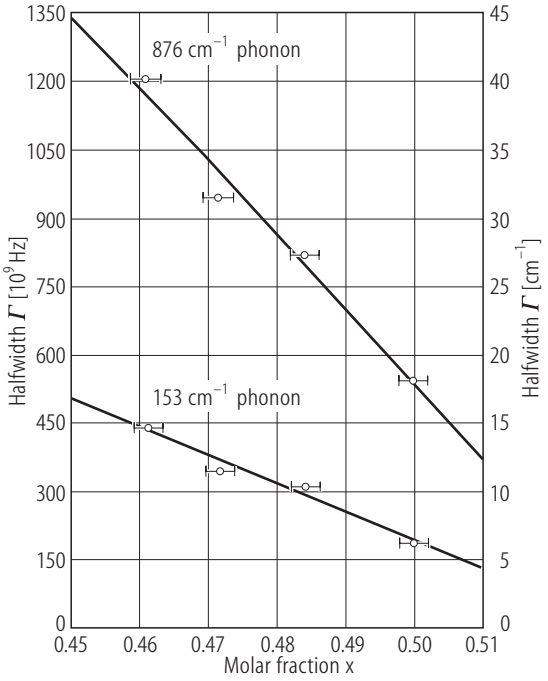

Fig. 2A-1-102. $LiNbO_3$. Γ vs. x [93Sch2]. Γ: halfwidths of the Raman lines at 153 cm^{-1} and 876 cm^{-1}. x: Li content.

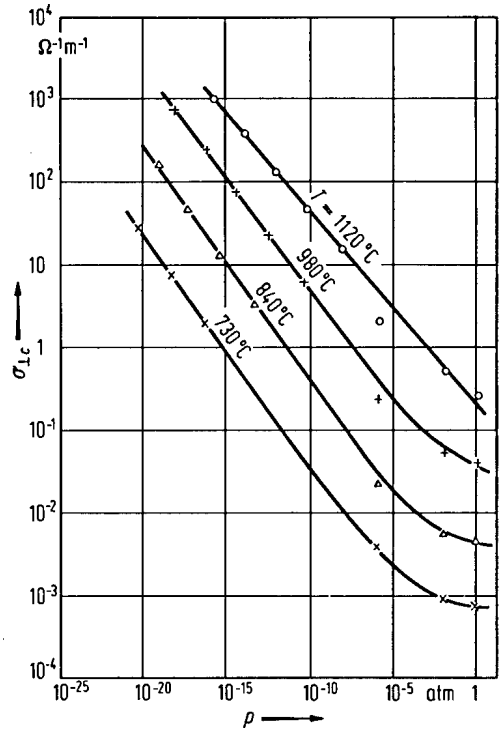

Fig. 2A-1-103. $LiNbO_3$. $\sigma_{\perp c}$ vs. p [68Ber]. p: oxygen partial pressure of ambient gas. 1 atm = 101325 Pa. Parameter: T.

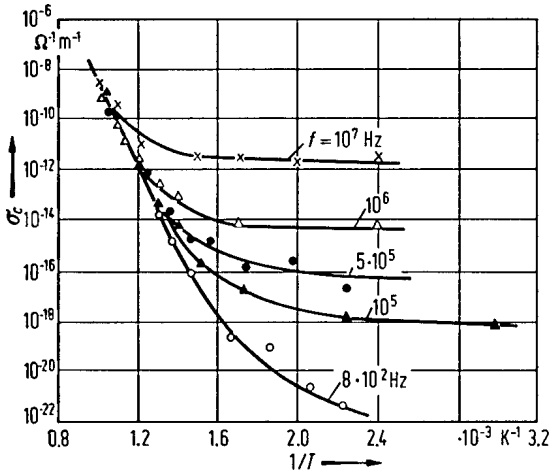

Fig. 2A-1-104. $LiNbO_3$. σ_c vs. $1/T$ [71Glu]. Parameter: f.

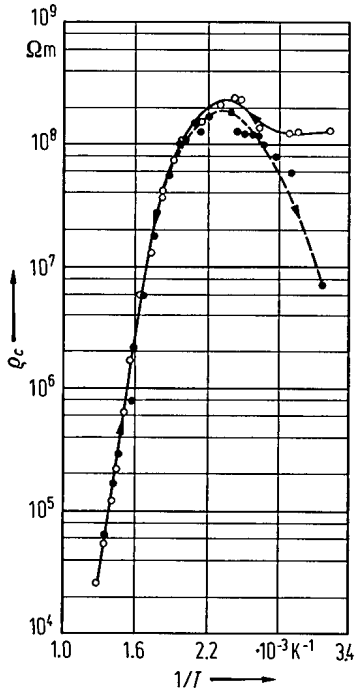

Fig. 2A-1-105. $LiNbO_3$. ρ_c vs. $1/T$ [78Kau].

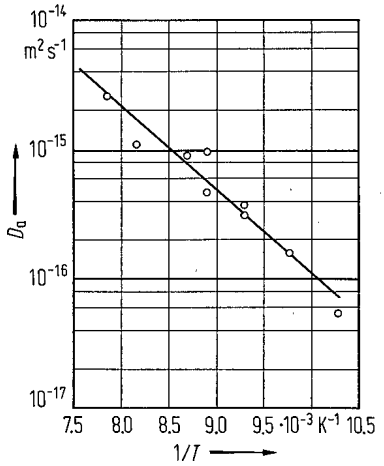

Fig. 2A-1-106. $LiNbO_3$. D_a vs. $1/T$ [69Jor]. D_a: oxygen diffusion coefficient along the *a*-axis. $D_c \approx D_a$.

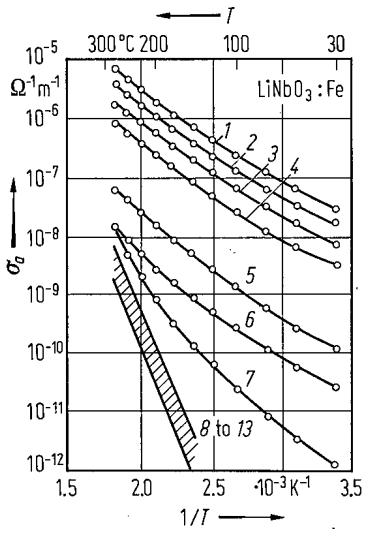

Fig. 2A-1-107. $LiNbO_3$. σ_a vs. $1/T$ [77Bar]. σ_a: conductivity of Fe doped single-domain crystals along the *a*-axis. Parameter: concentration of Fe dopants in wt %. *1*: 0.75, *2*: 0.65, *3*: 0.5, *4*: 0.44, *5*: 0.3, *6*: 0.25, *7*: 0.18, *8*: 0.1, *9*: 0.08, *10*: 0.057, *11*: 0.018, *12*: 0.014, *13*: 0.004.

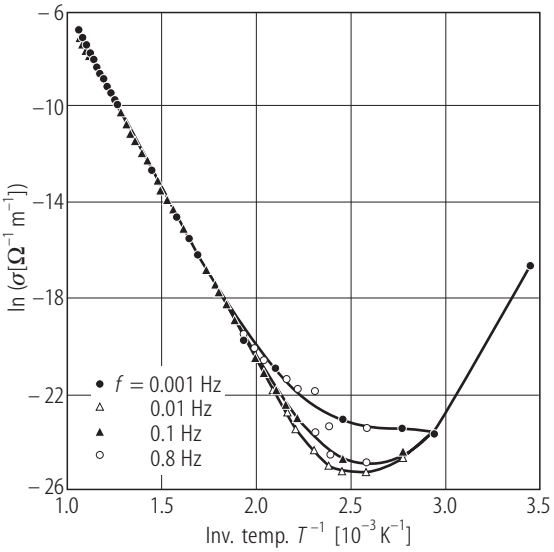

Fig. 2A-1-108. $LiNbO_3$. $\ln\sigma$ vs. $1/T$ [92Bak1]. σ: conductivity of a cleaved crystal. Parameter: *f*.

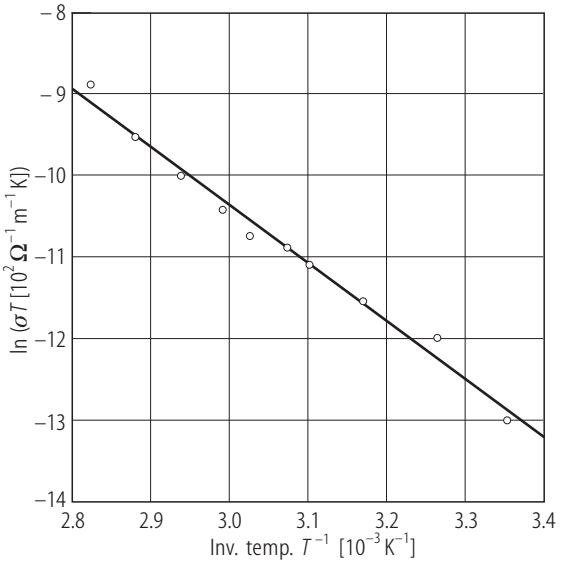

Fig. 2A-1-109. $LiNbO_3$ (thin film). $\ln(\sigma T)$ vs. $1/T$ [92Ben]. Sample: thin film prepared by RF sputtering. σ: electric conductivity.

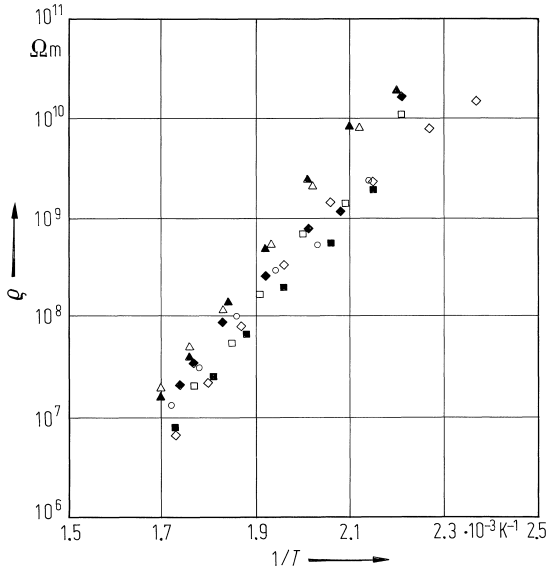

Fig. 2A-1-110. $LiNbO_3$ (undoped and Mg-, Fe-doped). ρ vs. $1/T$ [86Ger]. Open circles: commercial optical quality; open and full squares: floating zone purified; open and full triangles: 5 mol% MgO-doped; open diamonds: 5 mol% MgO-doped and 100 ppm Fe; full diamonds: 5 mol% MgO-doped and 200 ppm Fe.

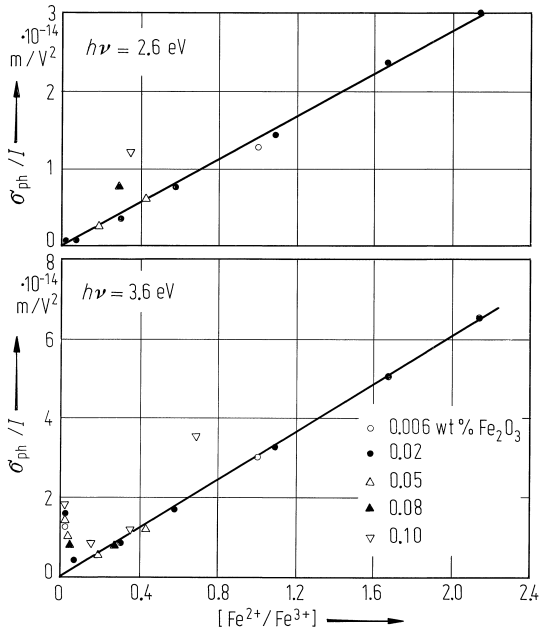

Fig. 2A-1-111. $LiNbO_3$ (Fe-doped). σ_{ph}/I vs. [Fe^{2+}/Fe^{3+}] [78Kra]. σ_{ph}: photoconductivity, I: irradiated light intensity, [Fe^{2+}/Fe^{3+}]: Fe ions concentration ratio. Parameter: Fe doping level.

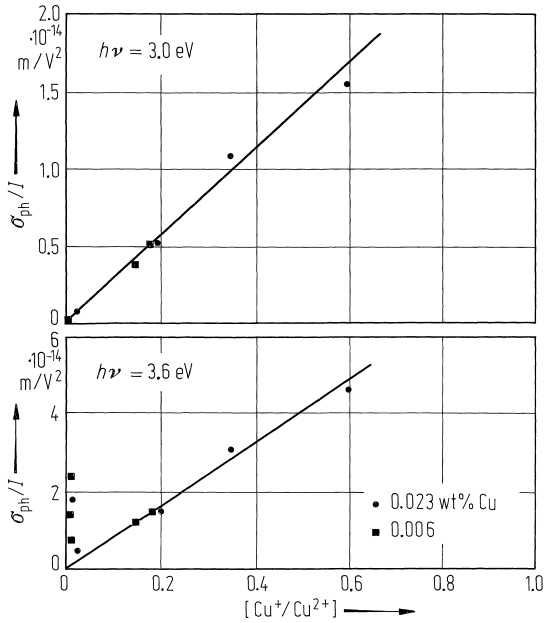

Fig. 2A-1-112. $LiNbO_3$ (Cu-doped). σ_{ph}/I vs. $[Cu^+/Cu^{2+}]$ [80Kra]. σ_{ph}: photoconductivity, I: irradiated light intensity, $[Cu^+/Cu^{2+}]$: Cu ions concentration ratio. Parameter: Cu doping level.

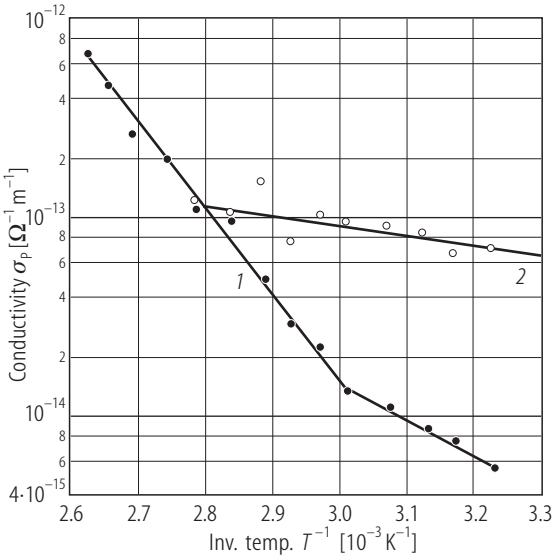

Fig. 2A-1-113. $LiNbO_3$. $\log\sigma_p$ vs. $1/T$ [86Bli]. σ_p: photoconductivity. Curve *1*: in the dark; *2*: with light illumination.

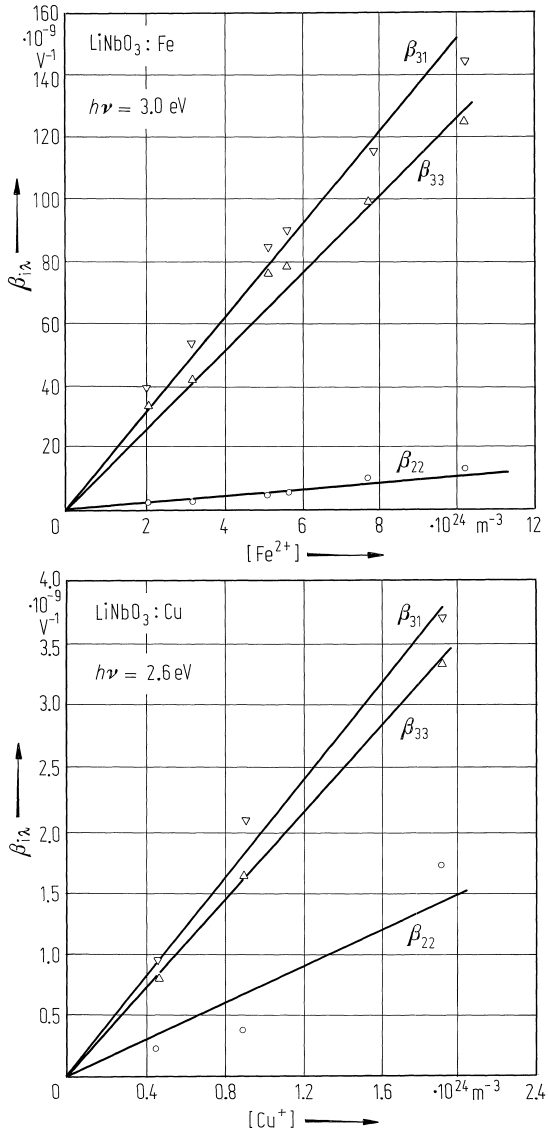

Fig. 2A-1-114. $LiNbO_3$ (Fe- and Cu-doped). $\beta_{i\lambda}$ vs. [*M*] [82Fes]. $\beta_{i\lambda}$: photovoltaic tensor component, [*M*]: doped ion concentration. $\beta_{i\lambda}=\beta_{ijk}$. β_{ijk} is defined by the equation $j_i/I = \beta_{ijk}e_je_k$, where j_i is a component of photovoltaic current density, I is the light intensity and e_j is a polarization vector component of the light.

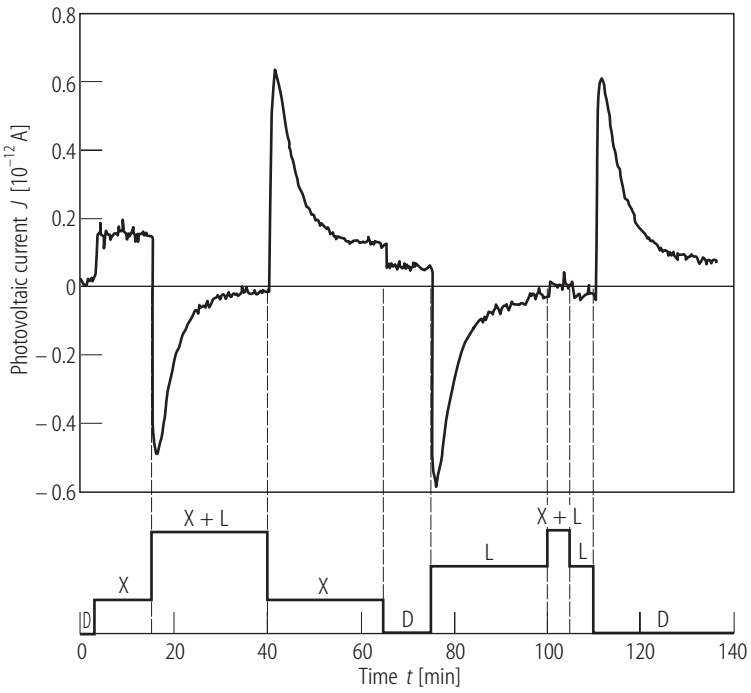

Fig. 2A-1-115. $LiNbO_3$. *J* vs. *t* [93Fri]. *J*: photovoltaic current. Irradiation: X-rays at 4 keV (X); visible light (L); combined excitation (X+L); darkness (D).

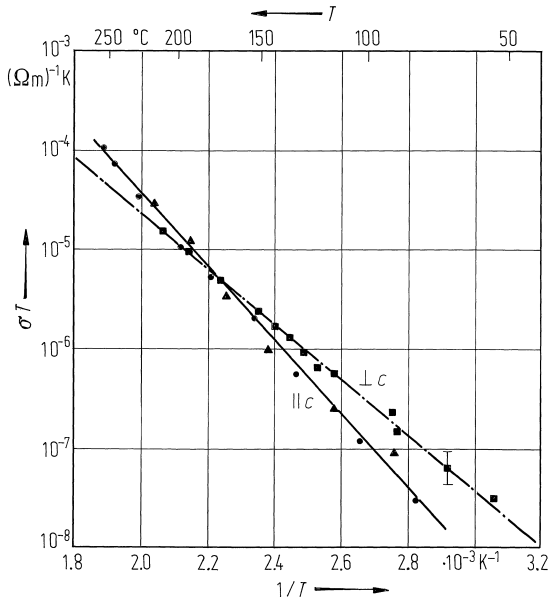

Fig. 2A-1-116. $LiNbO_3$. σT vs. $1/T$ [84Fra]. σ: dc Li^+ ionic conductivity. Circles: $\parallel c$ in vacuum, triangles: $\parallel c$ in argon, squares: $\perp c$. Li/Nb = 48.6/51.4.

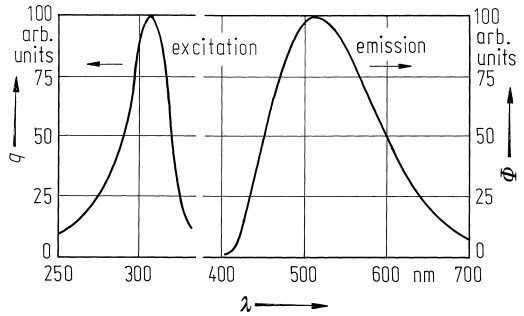

Fig. 2A-1-117. $LiNbO_3$. Photoluminescence spectrum at 5 K [80Kro]. *q*: relative quantum output, Φ: radiation power per constant wavelength interval. For the excitation spectrum λ_{exc} = 275 nm, for the emission spectrum λ_{em} = 500 nm.

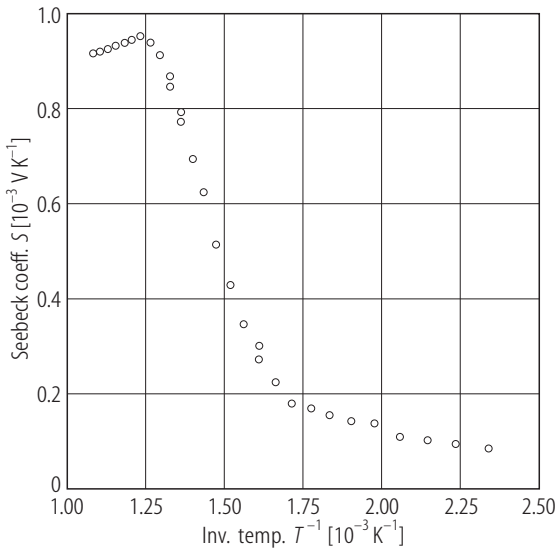

Fig. 2A-1-118. $LiNbO_3$. S vs. $1/T$ [92Bak2]. S: Seebeck coefficient.

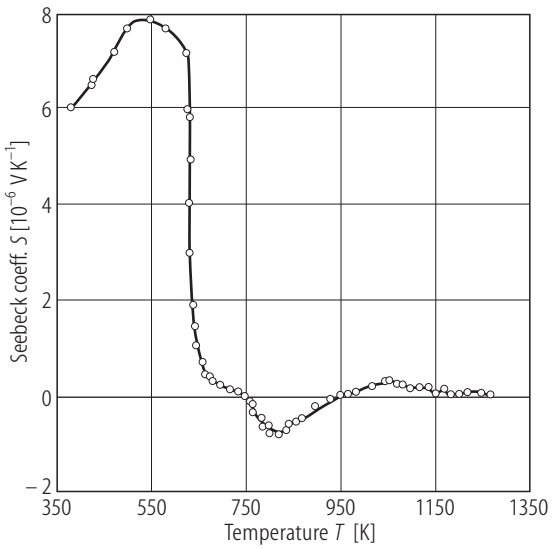

Fig. 2A-1-119. $LiNbO_3$. S vs. T [88Kha]. S: Seebeck coefficient.

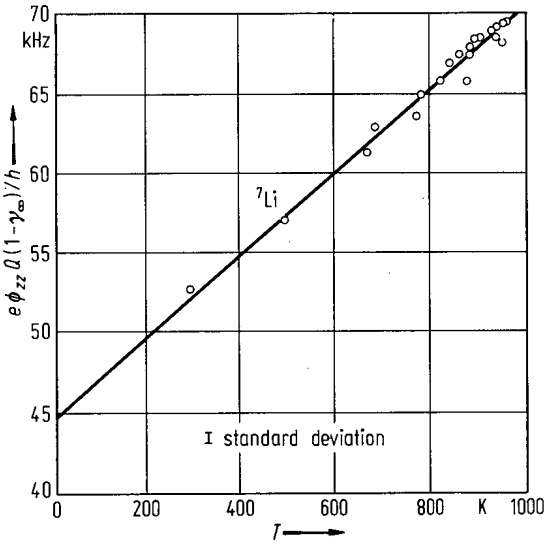

Fig. 2A-1-120. $LiNbO_3$. $e\phi_{zz}Q(1-\gamma_\infty)/h$ vs. T for ^{7}Li NMR [70Hal]. γ_∞: Sternheimer antishielding factor. $1-\gamma_\infty = 0.7448$.

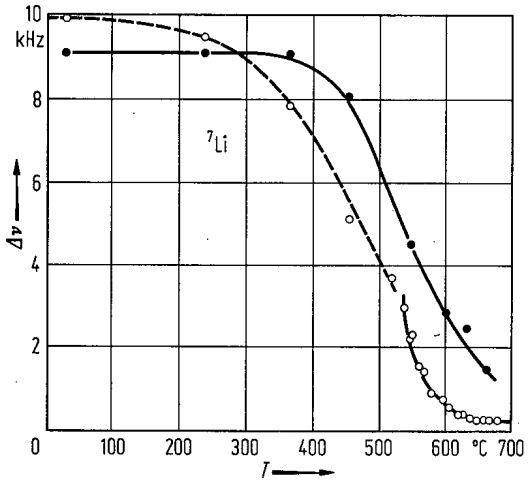

Fig. 2A-1-121. $LiNbO_3$. $\Delta\nu$ vs. T for ^{7}Li NMR [70Hal]. $\Delta\nu$: linewidth. Open circles: central line, full circles: satellite line.

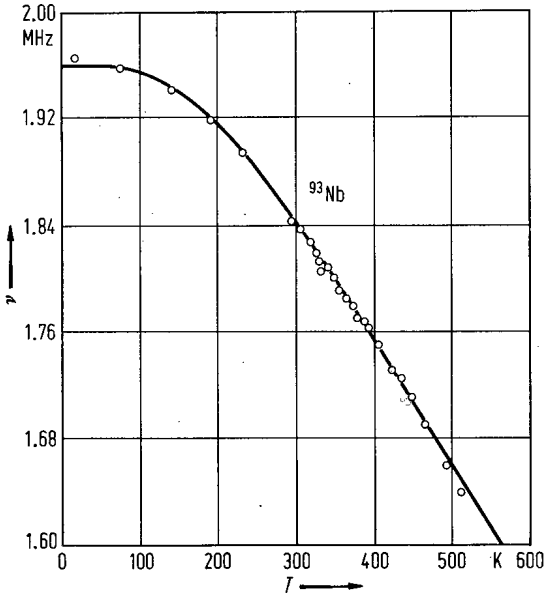

Fig. 2A-1-122. $LiNbO_3$. ν vs. T for ^{93}Nb NMR [70Sch]. ν: transition frequency for $m = 5/2 \leftrightarrow m = \pm 3/2$ transition.

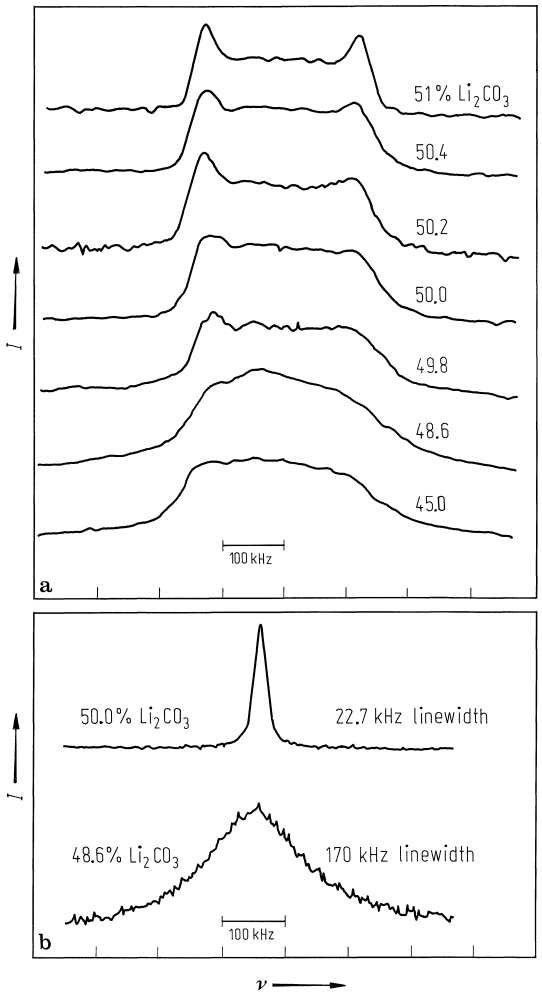

Fig. 2A-1-123. $LiNbO_3$. ^{93}Nb NMR spectra [86Dou]. (**a**) $1/2 \leftrightarrow -1/2$ transition of ceramic samples, f = 48.5 MHz; (**b**) $1/2 \leftrightarrow 3/2$ transition in single crystals, f = 49.42 MHz. $H \perp c$. Parameter: Li_2CO_3 mol% in the starting materials.

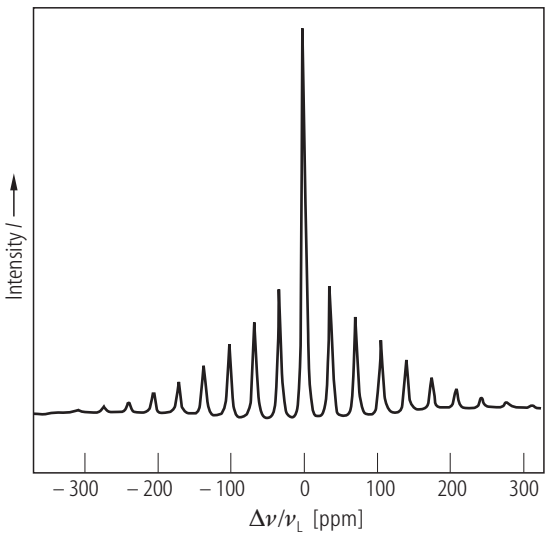

Fig. 2A-1-124. $LiNbO_3$. ^7Li MAS-NMR spectrum [94Blu]. *I*: signal intensity. Powder sample. ν_L = 116.6 MHz. MAS: magic angle spinning.

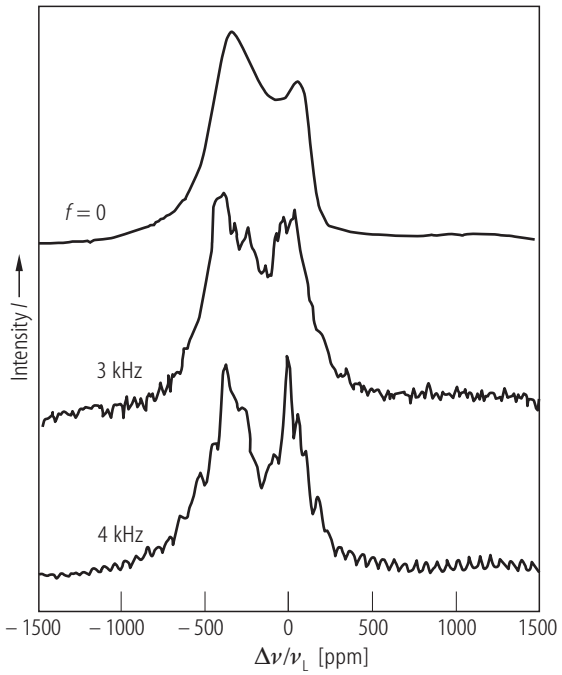

Fig. 2A-1-125. $LiNbO_3$. ^{93}Nb MAS-NMR spectrum [94Blu]. *I*: signal intensity. Powder sample. ν_L = 73.5 MHz. Parameter: spinning frequency of the sample. MAS: magic angle spinning.

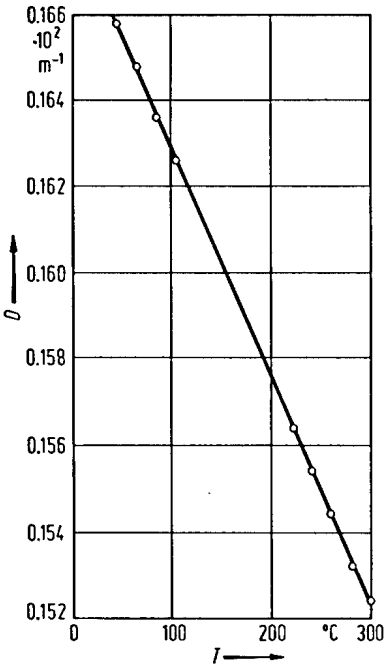

Fig. 2A-1-126. $LiNbO_3$:Fe^{3+}. *D* vs. *T* [72Meh2]. *D*: second order spin Hamiltonian parameter determined by ESR.

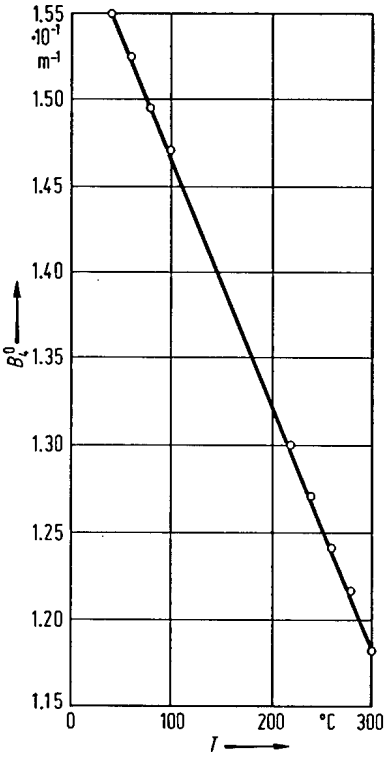

Fig. 2A-1-127. $LiNbO_3$:Fe^{3+}. B_4^o vs. T [72Meh]. B_4^o: fourth order spin Hamiltonian parameter determined by ESR.

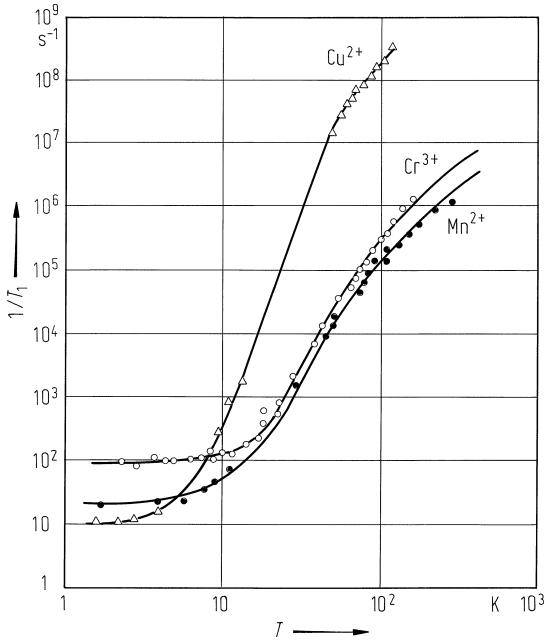

Fig. 2A-1-128. $LiNbO_3$. $1/T_1$ vs. T [84Kor]. T_1: spin-lattice relaxation time of Cu^{2+}, Cr^{3+}, Mn^{2+} ions. Transition: $-1/2 \leftrightarrow 1/2$. $H \parallel c$. $f \cong 9$ GHz.

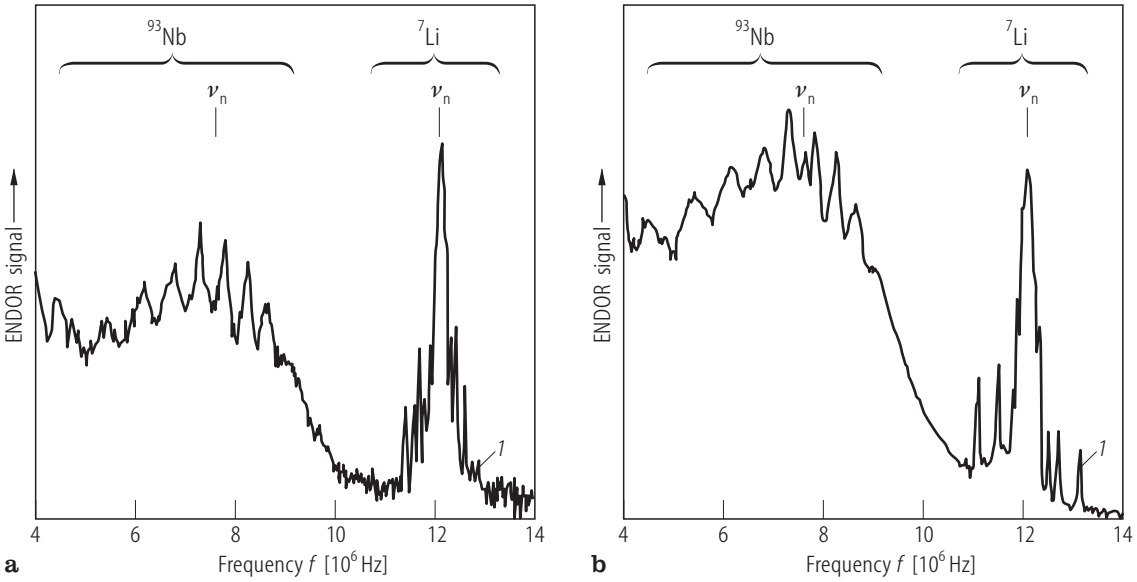

Fig. 2A-1-129. $LiNbO_3$:Fe^{3+}. ENDOR spectrum [92Sot]. H_0 = 7300 Oe. T = 4.5 K. (**a**) $H_0 \parallel y$, (**b**) $H_0 \parallel x$. ν_n: central frequency for nucleus.

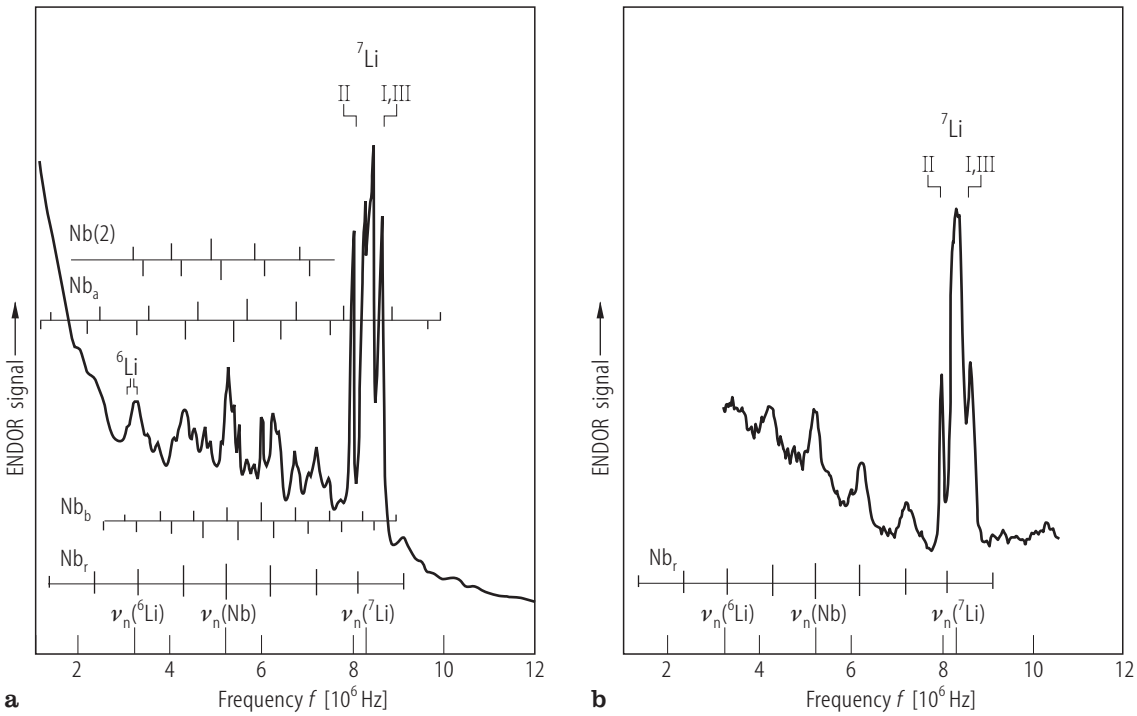

Fig. 2A-1-130. $LiNbO_3$:Mn^{2+}. ENDOR spectrum of Mn^{2+} centers [90Cor]. $H \parallel c$. H = 500.4 mT. T = 8 K. ν_n: central frequency for nucleus. (**a**) Stoichiometric crystal. Nb_a: on axis; Nb_b: neighbors; Nb_r: remote; Nb(2): off axis. (**b**) Congruent crystal. Nb_r: remote nuclei.

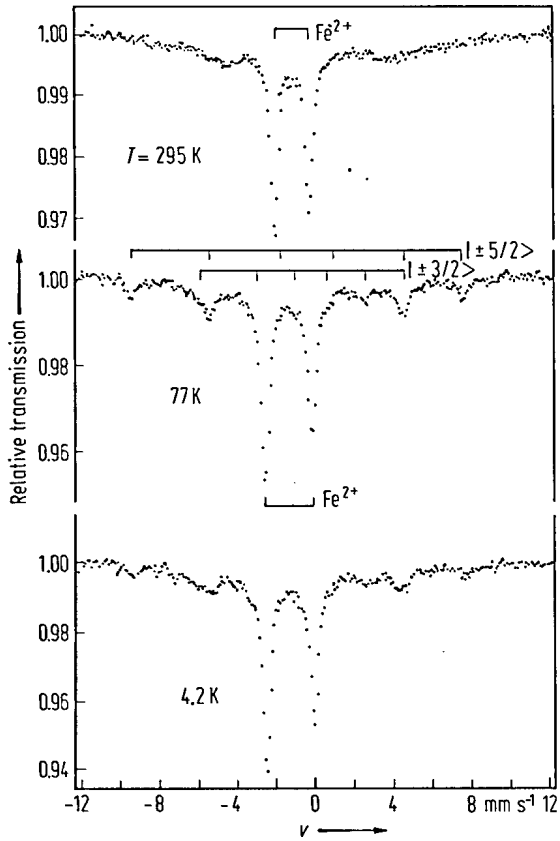

Fig. 2A-1-131. $LiNbO_3$:^{57}Co. Mössbauer spectra [75Keu]. v: source velocity. As absorbers, enriched $Na_4Fe(CN)_6 \cdot 10\ H_2O$ is employed at 295 K, and ^{57}Fe in Nb foil at 77 K and 4.2 K. The *c*-axis is perpendicular to the γ-ray direction.

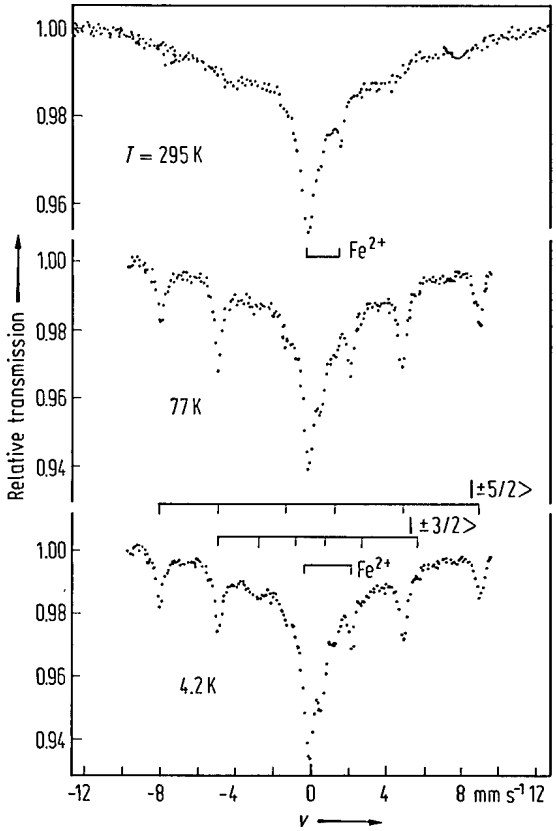

Fig. 2A-1-132. $LiNbO_3$:^{57}Fe. Mössbauer spectra [75Keu]. v: absorber velocity in original preparation state. ^{57}Co in Pd matrix is served as a source. Estimated Fe concentration is about 0.1 at %. The *c*-axis is perpendicular to the γ-ray direction.

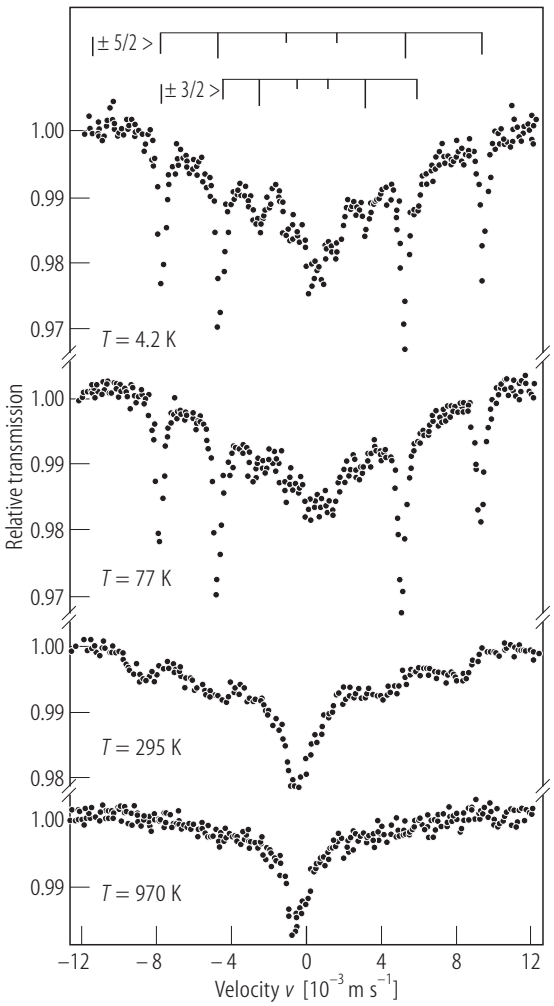

Fig. 2A-1-133. $LiNbO_3$:Fe. ^{57}Fe Mössbauer spectra [88Eng]. Sample: single crystal oxidized in air for 24 h at 300 °C. Parameter: *T*.

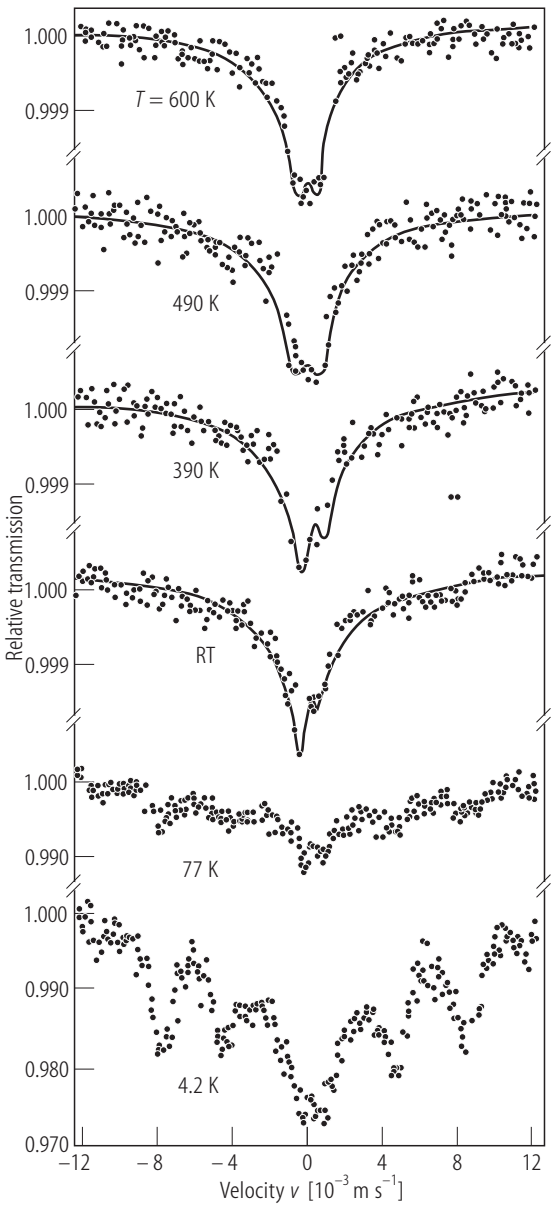

Fig. 2A-1-134. $LiNbO_3$:Fe. ^{57}Fe Mössbauer spectra [88Eng]. Sample: amorphous $LiNbO_3$ oxidized for 24 h in air at 300 °C. Parameter: *T*.

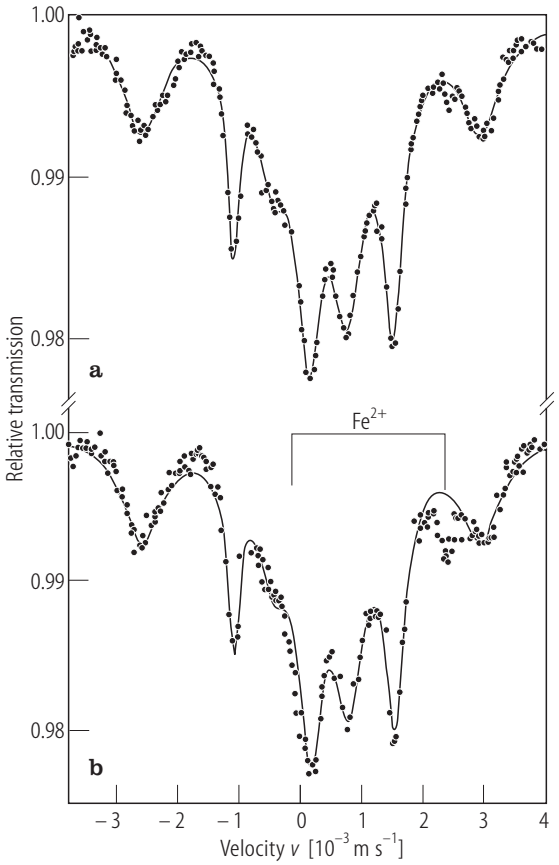

Fig. 2A-1-135. $LiNbO_3$:Fe. ^{57}Fe Mössbauer spectra at 4.2 K [88Eng]. Sample: a fully oxidized $LiNbO_3$. (**a**): before the light irradiation; (**b**): after the light irradiation (λ = 366 nm).

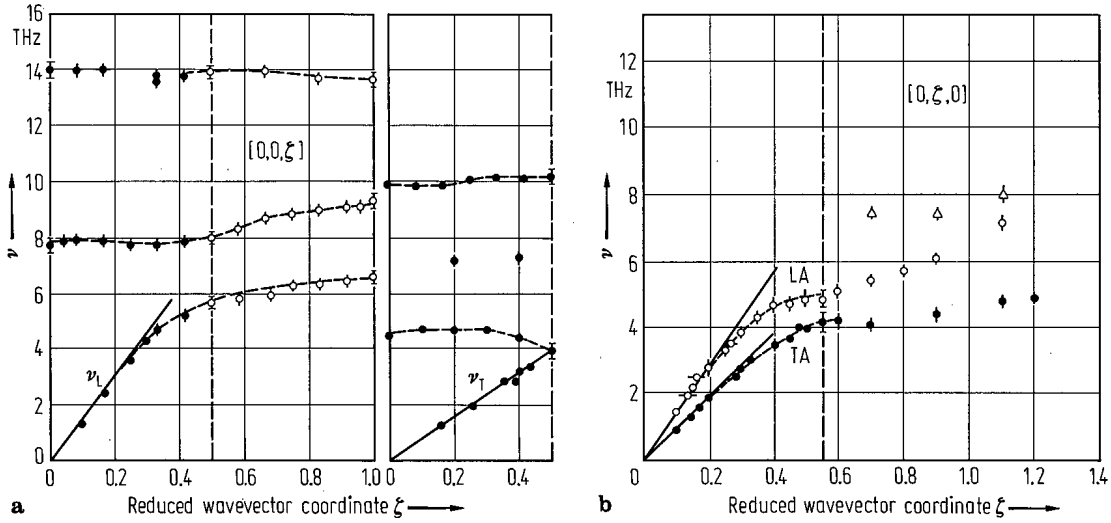

Fig. 2A-1-136. $LiNbO_3$. Phonon dispersion relations, (**a**) along the [001] directions (q = [0,0,ζ]·6π/c), and (**b**): along the [010] directions (q = [0,ζ,0]·4π / $\sqrt{3}a$) at 295 K [78Cho]. ν: frequency. The broken curves drawn through the experimental points are only for a guide. The solid lines represent the sound velocities.

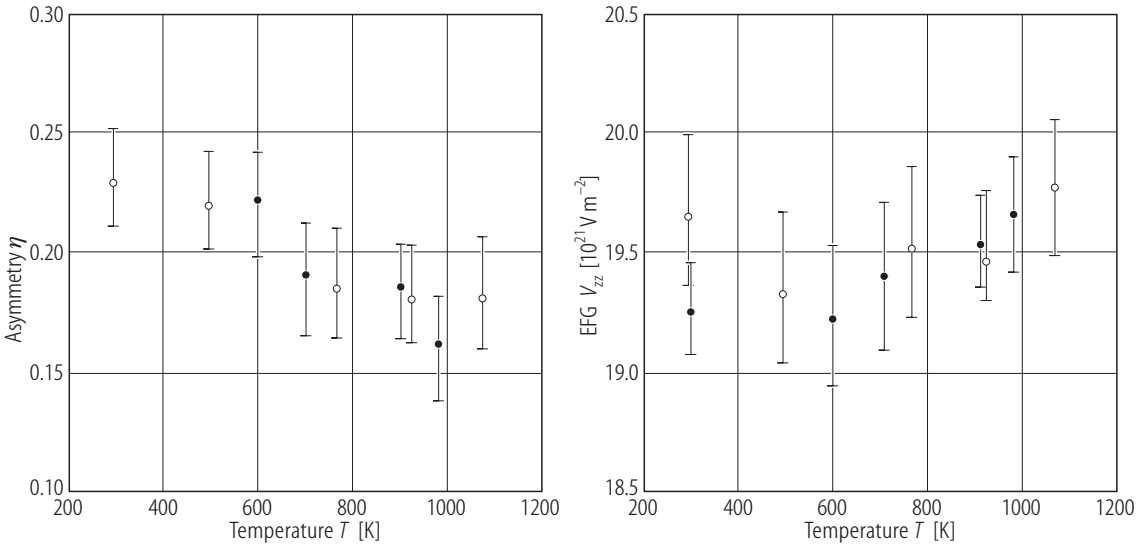

Fig. 2A-1-137. $LiNbO_3$. V_{zz}, η vs. T [91Cat2]. V_{zz}, η: electric field gradient and asymmetry parameter at Li sites determined by $^{181}Hf \rightarrow {}^{181}Ta$ perturbed-angular correlation spectroscopy.

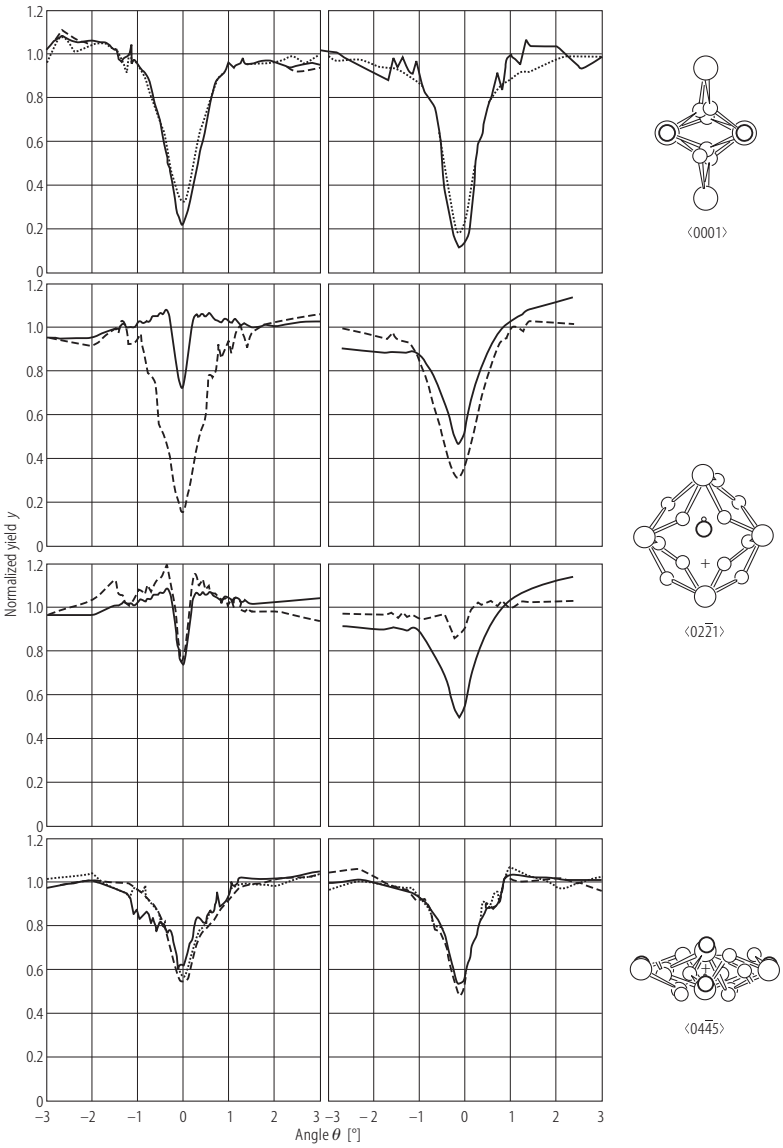

Fig. 2A-1-138. $LiNbO_3$:Ti. Comparison of experimental angular PIXE, RBS and NRA yield profiles [92Kol]. PIXE: particle induced X-ray emission. RBS: Rutherford backscattering. NRA: nuclear reaction analysis. *y*: normalized yield; θ: angle relative to the axis. Upper row: <0001> axis (*c*-axis) for the Ti-diffused $LiNbO_3$ crystal. Left: PIXE with 3.1 MeV He ions, (full line) Ti(K), (dotted line) Nb(K), (dashed line) Nb(L), the Nb(L) yield curve coincides for most data points with the Ti(K) curve. Right: RBS and NRA with 1.77 MeV protons, RBS (dotted line) Nb, NRA (full line) $^7Li(p, \alpha)^4He$. Second and third row from above: $\langle 02\bar{2}1 \rangle$ axis for 1.77 MeV protons. Left: 3 mol% Ti bulk doped $LiNbO_3$ crystal. Right: Ti-diffused $LiNbO_3$ crystal. Second row: PIXE (full lines) Ti(K), (dashed lines) Nb(L). Third row: PIXE (full lines) Ti(K), NRA (dashed lines) $^7Li(p, \alpha)^4He$. Lowest row: $\langle 04\bar{4}5 \rangle$ axis, PIXE with He ions (full lines) Ti(K), (dotted lines) Nb(K), (dashed lines) Nb(L). Left: 3 mol% Ti bulk doped $LiNbO_3$ crystal. Right: Ti-diffused $LiNbO_3$ crystal. At the right side projections on the corresponding axes are depicted, where the large circles symbolize Nb atoms, the smallest circles represent O and the medium size circles stand for Li. The cross represents the interstitial intrinsic octahedral site. Bonds between O and Nb atoms are represented by rods.

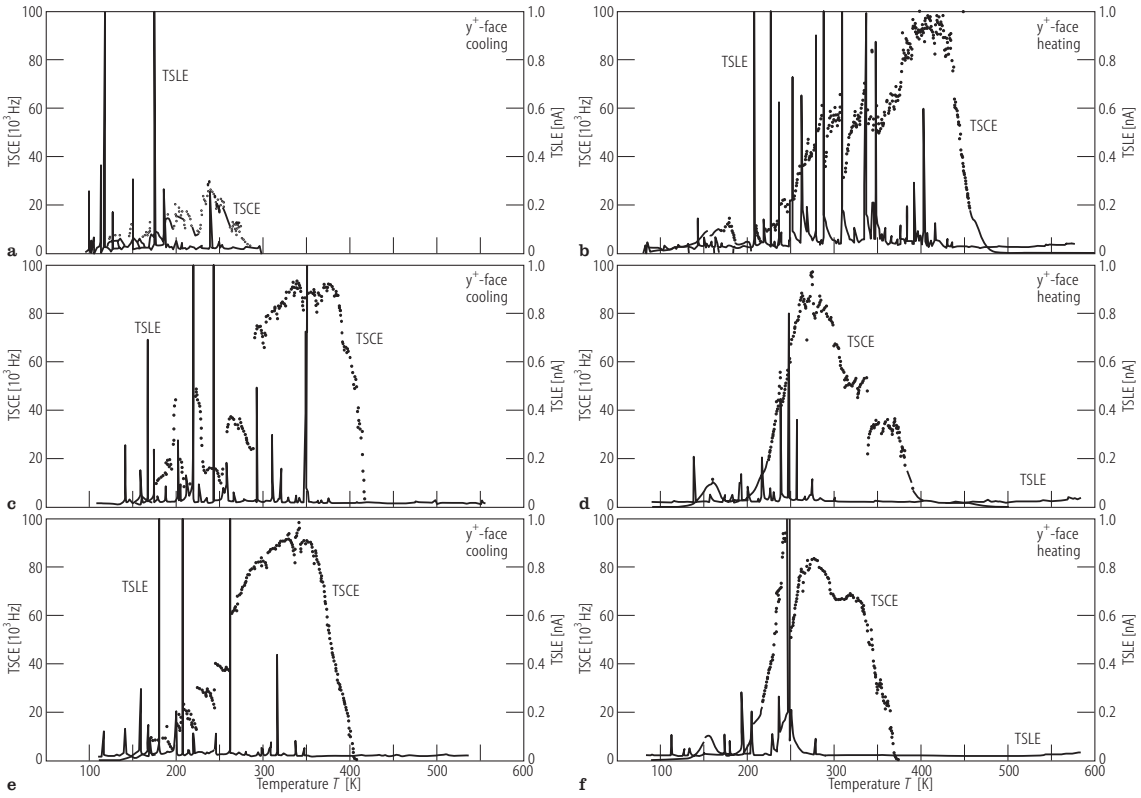

Fig. 2A-1-139. $LiNbO_3$. TSCE and TSLE vs. T [92Tom]. TSCE: thermally stimulated charge emission; TSLE: thermally stimulated light emission. Y^+-face. Measurements were done in alphabetical order indicated in the figure.